

# Constraints on Be star geometry derived from combined photometric, IR excess, and optical polarimetry data

C. Aerts<sup>1</sup> and G. Molenberghs<sup>2</sup>

<sup>1</sup> Instituut voor Sterrenkunde, Katholieke Universiteit Leuven, Celestijnenlaan 200 B, B-3001 Heverlee, Belgium

<sup>2</sup> Biostatistics, Limburgs Universitair Centrum, Universitaire Campus, Building D, B-3590 Diepenbeek, Belgium

Received 26 May 1994 / Accepted 21 July 1994

**Abstract.** Many attempts have already been made to propose a global physical model for a Be star by compiling separate studies (see e.g. Coté & Waters 1987; Waters 1993, among others). Unfortunately, photometric studies are usually left out of these syntheses. We here combine four different kinds of observations (photometric period, rotation velocity, intrinsic linear polarisation in the visual and IR excess) to see if they contain compatible information. From this study, we try to put constraints on the geometry of the stellar disc.

We find that the IR colour excess is not correlated to the photometric variability, contrary to the polarisation. The latter shows equal correlations with  $v \sin i$  and its square, indicating that the polarisation is an equally important function of  $\sin i$  and  $\sin^2 i$ . The relation between the photometric period and the polarisation indicates a possible link between stellar pulsation and mass loss. We stress, however, that our results are based on a very limited number of stars (14).

**Key words:** polarization – methods: statistical – stars: Be – stars: circumstellar matter – infrared: stars

## 1. Introduction

The Be stars are a group of B-type stars that show, or have shown in the past, emission lines in their spectrum. These emission lines are observed in the optical and IR spectrum and are caused by the presence of a cold, dense circumstellar envelope of ionised material. The presence of such a stellar envelope indicates that the Be stars eject much more material compared to “normal” B stars. The observed linear polarisation clearly indicates that the stellar wind of Be stars is non-spherically symmetric but has a disc-like geometry. It is clear that the rapid rotation is one of the most important effects that leads to the mass loss, but it cannot fully explain the circumstellar configuration. Indeed, other B stars exist that rotate more rapidly than some Be stars, while they do not show evidence for the presence of circumstellar material. Different models have by now been

suggested to be responsible and/or representative for the disc of Be stars (see e.g. Waters 1986, 1993; Bjorkman & Cassinelli 1993; Owocki et al. 1994).

In this research note, we first briefly discuss the results of the photometric analysis presented by Balona (1990) and of the IR study presented by Coté & Waters (1987) in Sect. 2; we also list the stars in common in their data sets. In Sect. 3, we present a canonical correlation analysis applied to the intersection of the data sets. This statistical technique was especially developed to study the intervariability of two data sets that have been obtained with completely different methods. Finally, we give some implications of our findings on the stellar geometry of Be stars and compare them with the already proposed models in Sect. 4.

## 2. The data

### 2.1. The photometric data

From an extensive study of the short-period variability of 60 southern Be stars, Balona (1990) reports a significant correlation between the projected rotation velocity  $v \sin i$  and the photometric frequency  $f$ . Such a correlation tends to indicate that the periodic light variations are due to rotating stellar spots and not to non-radial pulsations. The latter, however, are often claimed to be the mechanism responsible for the variability and the mass loss in Be stars (e.g. Vogt & Penrod 1983; Baade 1984, 1987). As long as multiperiodicity cannot be convincingly shown, both models are viable.

If the photometric period is identical to the rotation period, then an estimate of the stellar radius enables a determination of the equatorial rotation velocity and thus also of the inclination angle. Unfortunately, estimates of the radii of Be stars are very imprecise. Therefore, we think that no clear distribution of  $\sin i$  can be obtained in this way.

In his analysis, Balona used  $v \sin i$ -values mostly obtained from the Bright Star Catalogue. We have added the stars listed in Cuypers et al. (1989) and in Balona et al. (1992) that were not present in the 1990 data set and considered only those stars for

which  $v \sin i$ -values and periods were obtained. This resulted in 40 objects.

## 2.2. The IRAS data

The presence of circumstellar material around hot stars can be detected in the IR as an excess of IR radiation relative to the expected photospheric continuum flux. The IR excess observed in hot stars is due to free-bound and free-free radiation from the stellar wind and gives information on the density structure of the circumstellar material (see e.g. Waters 1986). In a statistical study of the IR excess of 101 Be stars based on IRAS observations, Coté & Waters (1987) describe a number of relationships of the  $12\mu$  IR colour excess with stellar parameters.

In their study of the  $12\mu$  IR colour excess versus intrinsic linear polarisation (obtained for 45 stars from McLean & Brown 1978), Coté & Waters find a clear “triangle-shaped” distribution with a well-defined upper limit given by

$$P = 0.83CE(V, [12]), \quad (1)$$

where  $P$  is the polarisation at  $4250\text{ \AA}$  in percent and  $CE(V, [12])$  is the IR colour excess at  $12\mu$ . The authors did not find a clear relation between  $v \sin i$  and the position of the star in the triangle-shaped distribution, although  $P$  is proportional to  $\sin^2 i$  for optically thin discs (see e.g. McLean & Brown 1978; Waters 1986). In a later paper, this conclusion is confirmed by Waters & Marlborough (1992), who also showed that  $P$  is no longer proportional to  $\sin^2 i$  for optically-thick discs.

In their analysis, Coté & Waters used  $v \sin i$ -values of Slettebak (1982), who presents a homogeneous study of the rotation velocities of 183 Oe, Be, and A–F type shell stars over the entire sky. We have therefore chosen to consider his  $v \sin i$ -values; if the  $v \sin i$ -values were not available in Slettebak’s data set, we kept the value adopted by Balona (1990).

## 2.3. The intersection of the two data sets

The four parameters  $f$ ,  $v \sin i$ ,  $CE(V, [12])$ , and  $P$  are unfortunately only available for 14 stars common to the data sets. In Table 1, we list these 14 objects and the values of the four parameters together with the spectral type. Although 14 objects is a very small sample, we could recover the relationship between  $f$  and  $v \sin i$  as found by Balona (1990). A plot of  $f$  versus  $v \sin i$  for the 14 objects in the intersection of the two data sets is given in Fig. 1. Also the triangle-shaped distribution found by Coté & Waters (1987) is rather well recovered with the 14 objects, as can be seen in Fig. 2. The full line in the figure is the upper limit given by Exp. (1). It is clear from this figure that  $\epsilon$  Cap has an extremely large polarisation for its  $12\mu$  colour excess. Since both known relations are well recovered, we assume that the 14 stars form a representative sample taken at random from the class of Be stars, but we keep in mind that the results of our analysis might be altered when more stars are available in the sample.

In the following section, we study possible associations between  $f$ ,  $v \sin i$ ,  $CE(V, [12])$ , and  $P$ . Moreover, we investigate

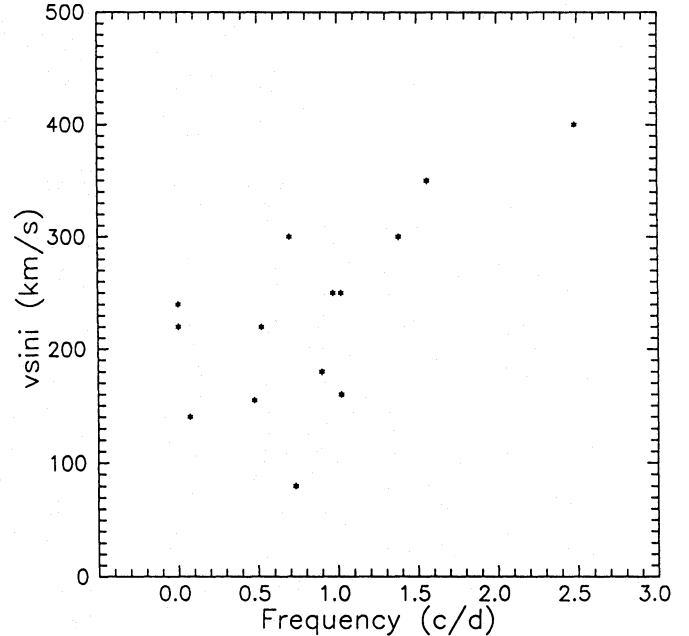


Fig. 1. An  $f$  versus  $v \sin i$  plot of the 14 objects presented in Table 1

whether or not the photometric and IRAS analyses yield compatible information and if so, if we can put constraints on the geometry of the disc by combining the results obtained with each of the methods separately.

## 3. Canonical correlation analysis

### 3.1. Outline of the method

Suppose we have a set of measurements on each of  $n$  objects, naturally falling apart into two subsets of measures (here: the photometric and IRAS data sets). If we want to study the association between the two sets of variables, we could pick the pair of variables, one in each set, showing the highest correlation. However, this procedure is less meaningful if the initial variables have unequal variances and if there is also a correlation between the variables within each subset. The aim of canonical correlation analysis is to transform the variables in each set in order to maximise the between-set correlation and to facilitate the interpretation of that correlation.

To have a clear picture of the correlation between the two sets, we search for a pair of linear combinations of the initial variables, one in each set, that exhibit maximal correlation: the *canonical variables*. It is easy to show that this comes down to searching the eigenvalues (the square root of which are called *canonical correlations*) of a function of the component blocks of the correlation matrix of the data. Each of the original sets of variables is replaced by a set of canonical variables with unit variance, mutually orthogonal and pairwise uncorrelated.

If the  $n$  objects for which we compute the canonical correlations are drawn at random from a population having a multivariate normal distribution, then the canonical correlations and canonical variables computed from the sample are the maximum

**Table 1.** The 14 stars and their values for the frequency  $f$ , the projected rotation velocity  $v \sin i$ , the  $12\mu$  IR colour excess  $CE(V, [12])$ , and the intrinsic linear polarisation  $P$ . The spectral type is given in the last column. ( $^{\circ}$ ) indicates that a constant lightcurve has been detected.

Name	HR	HD	$f$ (c/d)	$v \sin i$ (km/s)	$CE(V, [12])$ (mag)	$P$ (%)	SpT
DX Eri	1508	30076	0.899	180	1.04	0.65	B2Ve
$\omega$ Ori	1934	37490	0.5097	160	1.90	0.5	B3IIIe
$\omega$ CMa	2749	56139	0.733	80	1.18	0.2	B2III-Ve
$\omega$ Car	4037	89080	0( $^{\circ}$ )	220	0.67	0.15	B8IIIe
$\delta$ Cen	4621	105435	0.52	220	1.94	0.42	B2IVne
$\mu$ Cen	5193	120324	0.4757	155	0.23	0.05	B2IV-Ve
$\eta$ Cen	5440	127972	1.563	350	0.83	0.5	B1.5IVne
48 Lib	5941	142983	2.4876	400	1.63	0.95	B5IIIpe
$\chi$ Oph	6118	148184	0.073	140	2.18	0.2	B2IVpe
$\alpha$ Ara	6510	158427	1.0194	250	2.25	0.7	B2Vne
66 Oph	6712	164284	0( $^{\circ}$ )	240	2.14	0.7	B2Ve
$\epsilon$ Cap	8260	205637	0.971	250	0.54	1.3	B2.5Vpe
$\omicron$ Aqr	8402	209409	0.6978	300	0.95	0.5	B7IVe
EW Lac	8731	217050	1.383	300	2.22	1.8	B4IIIpe

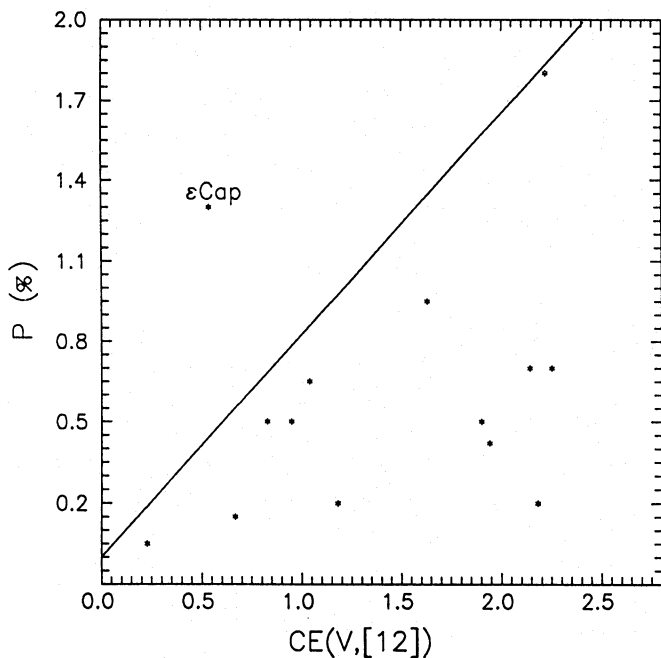


**Fig. 2.** A plot of the  $12\mu$  colour excess versus intrinsic linear polarisation for the 14 objects presented in Table 1. The full line is the upper limit found by Coté & Waters, given by Exp. (1)

likelihood estimates of the population canonical correlation and of the population canonical variables respectively, whence inference procedures apply. As the canonical correlations measure the between-set variability, we can test hypotheses about the number of canonical variables needed to appropriately describe the variability present in the population.

In order to study the correlation, we consider the largest eigenvalues and perform hypothesis tests to see whether these eigenvalues are significantly different from zero. If so, then in-

tervariability exists, if not then there is no between-set correlation. The simplest situation would be the one for which only one canonical variable is needed in each set to describe the inter-variability, i.e. when only the largest eigenvalue is significantly different from zero. For a detailed description of the method, we refer the reader to the books of Seber (1984), Johnson & Wichern (1988), and Krzanowski (1988).

### 3.2. Application to the data

A canonical correlation analysis is performed on the 14 stars in the intersection of the photometric and IRAS data sets. The first three variables pertain to Balona's correlation study ( $f, v \sin i, (v \sin i)^2$ ), while the remaining two stem from Coté & Waters' correlation study ( $P, CE$ ). Note that we have added  $(v \sin i)^2$  to the photometric study, since it is more likely that  $P$  is correlated with  $\sin^2 i$  than with  $\sin i$  from theoretical models. The analysis will show if this is really the case in practice.

The correlations between the variables are:

	$f$	$v \sin i$	$(v \sin i)^2$	$CE$	$P$
$f$	1.000	0.661	0.750	0.041	0.519
$v \sin i$	0.661	1.000	0.979	0.049	0.538
$(v \sin i)^2$	0.750	0.979	1.000	0.036	0.491
$CE$	0.041	0.049	0.036	1.000	0.230
$P$	0.519	0.538	0.491	0.230	1.000

First, we confirm the result of Balona (1990) as we find a correlation coefficient of 66 % between  $f$  and  $v \sin i$ . We also recover that there is no correlation between  $CE$  and  $v \sin i$ , as already mentioned by Coté & Waters (1987). Further, we see that the photometric variables correlate highly with  $P$ , but not at all with  $CE$ .

The eigenvalues  $R_i$  and canonical correlations  $R_i^2$  are displayed below.

$i$	$R_i$	std.e.	$R_i^2$
1	0.733	0.128	0.538
2	0.047	0.277	0.002

The first canonical correlation  $R_1^2$  is high, while the second one seems negligible. This indicates that the association between the two sets of variables can be captured completely by considering a single linear combination in each data set. This conclusion can be confirmed by performing hypothesis tests on the eigenvalues.

We would be interested in rejecting the hypothesis that the first canonical correlation is zero. This comes down to showing that between-set variability, based on the first canonical correlation, exists. The hypothesis test  $H_0: R_1 = 0$  is rejected at the 5% level, implying that between-set variability does indeed exist. It can also be shown that taking into account  $R_2$  adds nothing to the understanding of the between-set variability.

We now present the canonical variables for both sets in standardised version (i.e. all variables are dimensionless and have unit variance):

Standardised canonical coefficients  
for the photometric data

	$CV1(f, v \sin i, (v \sin i)^2)$	$CV2(f, v \sin i, (v \sin i)^2)$
$f$	1.118	-0.470
$v \sin i$	3.806	-4.377
$(v \sin i)^2$	-3.877	5.273

Standardised canonical coefficients  
for the IRAS data

	$CV1(CE, P)$	$CV2(CE, P)$
$CE$	-0.179	-1.032
$P$	1.039	0.136

The correlation between the first canonical variable of each set is given by the eigenvalue  $R_1$ , i.e.  $CV1(f, v \sin i, (v \sin i)^2)$  and  $CV1(CE, P)$  have a correlation of 73% (see Fig. 3). As can be seen from the contributions of  $P$  and  $CE$  to  $CV1(CE, P)$ ,  $CE$  plays a minor role. Thus,  $CV1(f, v \sin i, (v \sin i)^2)$  highly correlates with  $CV1(CE, P) \approx P$ .  $CV2(f, v \sin i, (v \sin i)^2)$  and  $CV2(CE, P)$  are virtually uncorrelated, as can be seen in Fig. 4.

Since  $P$  is far more important than  $CE$  to study the correlation between both sets, we have performed a canonical correlation analysis with the single variable  $P$  in the IRAS data set, which comes down to a multiple regression. The fitted regression model equals

$$P = -1.49(\pm 0.82) + 0.58(\pm 0.28)f + 0.015(\pm 0.007)v \sin i - 0.000032(\pm 0.000016)(v \sin i)^2,$$

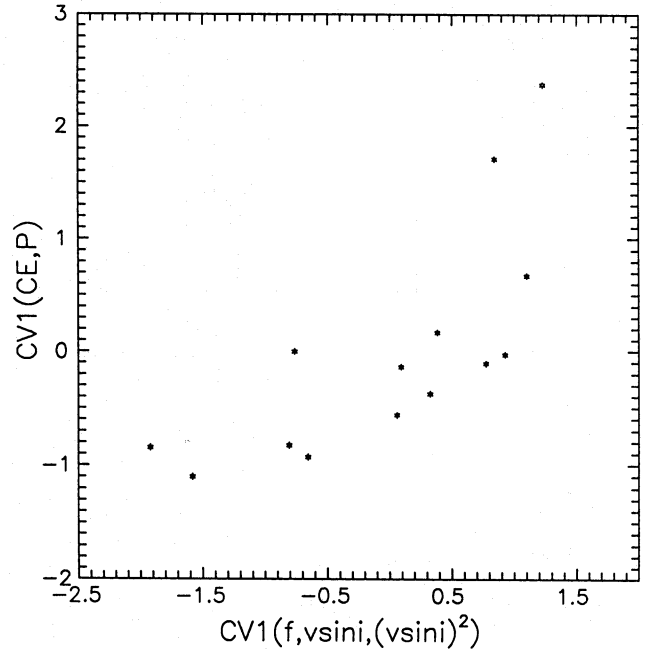


Fig. 3. A plot of the first canonical variable for the photometric data versus the first canonical variable for the IRAS data for the 14 stars.

where  $P$  is obtained in % if  $f$  is expressed in  $c/d$  and  $v \sin i$  in  $\text{km/s}$ . In standardised form, we obtain

$$P = 0.81(\pm 0.39)f + 2.79(\pm 1.27)v \sin i - 2.84(\pm 1.44)(v \sin i)^2.$$

This corresponds to a squared canonical correlation  $R^2 = 0.52$ . The corresponding hypothesis test  $H_0: R = 0$  has a P-value of 0.052 and is thus rejected at 10% level only. Also, the regression coefficients are significant at 10% level, but not at 5% level. This is probably due to the small sample size.

The spectral type dependence of the polarisation and the IR excess might alter our findings (Bjorkman & Cassinelli 1990). Therefore, we redid the entire analysis by considering the  $P$ - and  $CE$ -values from which we first removed the spectral dependence as described by Bjorkman (1992). This analysis did not yield different results as the ones described above.

#### 4. Discussion

From a canonical correlation analysis, we conclude that the photometric and IRAS data contain overlapping information, but also information that cannot be obtained with the other method. For example, contrary to the polarisation, the  $12\mu$  colour excess cannot be captured by  $f$  nor by  $v \sin i$ . Because the coefficients for  $v \sin i$  and  $(v \sin i)^2$  are of similar magnitude in the standardised form of the multiple regression, we can conclude that  $P$  is not a function of  $\sin^2 i$  only, but that it also contains an equally important contribution depending on  $\sin i$ .

The intersection of the photometric and the IRAS data reveals a rather strong correlation between  $P$  and respectively  $f$ ,  $v \sin i$ , and  $(v \sin i)^2$ . A large value for  $f$  (i.e. a short-period

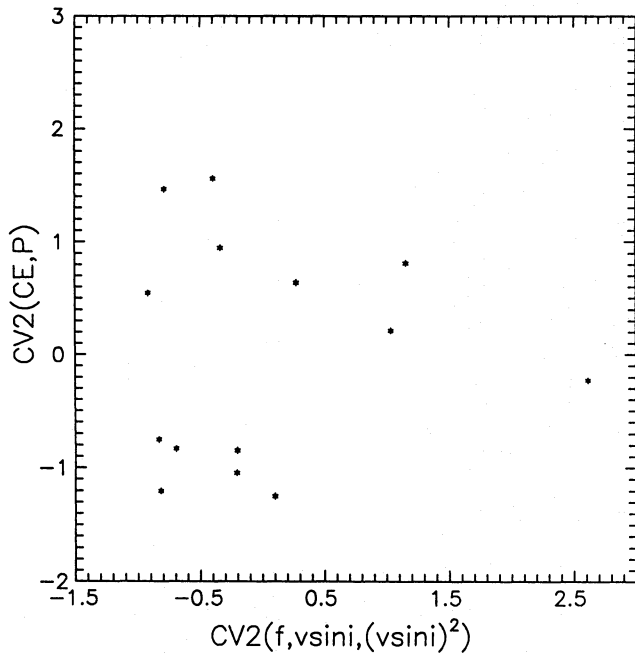


Fig. 4. A plot of the second canonical variable for the photometric data versus the second canonical variable for the IRAS data for the 14 stars.

photometric variation), typically corresponds to a large polarisation. If the rotational modulation hypothesis is correct, this implies a larger polarisation for rapid rotators. If, however, the photometric variability is due to non-radial pulsations, then we find that short-period non-radial modes imply a larger polarisation, and hence a more asymmetric density distribution around the star. A possible link between mass loss and pulsation has been suggested before (e.g. Owocki et al. 1988), but is not so easily explained from a theoretical point of view. Indeed, even if pulsations were to inject more mass in the lower wind, it should still be driven to infinity by the line-scattering force (Owocki, private communication).

The colour excess is not correlated to  $f$ ,  $v \sin i$ , and  $(v \sin i)^2$ . For the rotation velocity, this result was reported before (see e.g. Coté & Waters 1987) but it still is somewhat surprising. Indeed, in case of thin discs as produced by the wind compressed disc model (Bjorkman & Cassinelli 1993; Owocki et al. 1994) one expects a clear difference in colour excess between an edge-on and a pole-on configuration. The lack of correlation might be more compatible with the “wine-bottle” geometry recently proposed by Waters (1993, see his Fig. 4), since the IR excess could be produced at a large distance from the stellar photosphere. If this is the case, then it also explains why no correlation between  $f$  (typically representing changes in the stellar envelope) and  $CE$  is observed. It could also be that a  $\sin i$  dependence

does appear, but that it can only be found after the removal of the equatorial rotation velocity from  $v \sin i$  (Bjorkman, private communication). As already mentioned, we have considered the determination of the stellar radii to be too uncertain to give reliable results for  $\sin i$ .

We finally stress that our analysis is based on a very small number of objects (14). Adding more stars might alter our conclusions. More polarisation data exist, but at different wavelengths and/or obtained and reduced with different methods. However, to validate an analysis as presented here, it is extremely important that measurements are collected in exactly the same way for each star. Further, multivariate normality of the observations must hold, or at least a moderate to large sample size is required if the analysis is used for inferential procedures such as hypothesis testing. In the small sample case as presented here, the methods are still useful for exploring the data and to motivate further research.

*Acknowledgements.* We are grateful to Christoffel Waelkens for introducing us into this subject. We also thank John Bjorkman, Rens Waters, and Stan Owocki for helpful comments.

## References

- Baade, D. 1984, *A&A* 135, 101  
 Baade, D. 1987, In *Physics of Be stars*, eds. A. Slettebak & T.P. Snow, Cambridge University Press, p.361  
 Balona, L.A. 1990, *MNRAS* 245, 92  
 Balona, L.A., Cuypers, J., Marang, F. 1992, *A&AS* 92, 533  
 Bjorkman, J.E. 1992, PhD Thesis, University of Wisconsin, USA  
 Bjorkman, J.E., Cassinelli, J.P. 1990, In *Angular Momentum and Mass Loss for Hot Stars*, eds. L.A. Wilson & R. Stalio, Kluwer Academic Publishers, p.185  
 Bjorkman, J.E., Cassinelli, J.P. 1993, *ApJ* 409, 429  
 Coté, J., Waters, L.B.F.M. 1987, *A&A* 176, 93  
 Cuypers, J., Balona, L.A., Marang, F. 1989, *A&AS* 81, 151  
 Johnson, R.A., Wichern, D.W. 1988, *Applied Multivariate Statistical Analysis*, Prentice-Hall  
 Krzanowski, W.J. 1988, *Principles of Multivariate Analysis*, Clarendon Press, Oxford  
 McLean, I.S., Brown, J.D. 1978, *A&A* 69, 291  
 Owocki, S.P., Castor, J.I., Rybicki, G.B. 1988, *ApJ* 335, 914  
 Owocki, S.P., Cranmer, S.R., Blondin, J.M. 1994, *ApJ* 424, 887  
 Seber, G.A.F. 1984, *Multivariate Observations*, John Wiley & Sons  
 Slettebak, A. 1982, *ApJS* 50, 55  
 Vogt, S.S., Penrod, G.D., Hatzes, A.P. 1987, *ApJ* 496, 127  
 Waters, L.B.F.M. 1986, PhD Thesis, University of Utrecht, The Netherlands  
 Waters, L.B.F.M. 1993, In *IAU Symposium 162: Pulsation, Rotation and Mass Loss in Early-Type Stars*, Kluwer Academic Publishers, in press  
 Waters, L.B.F.M., Marlborough, J.M. 1992, *A&A* 256, 195